Inorganic Chemistry

Article

pubs.acs.org/IC

Photophysical Studies of Europium Coordination Polymers Based on a Tetracarboxylate Ligand

Yan-Li Gai,[†,‡] Fei-Long Jiang,[†] Lian Chen,[†] Yang Bu,[†,‡] Kong-Zhao Su,[†,‡] Shaeel A. Al-Thabaiti,[§] and Mao-Chun Hong*[,†]

[†]State Key Laboratory of Structure Chemistry, Fujian Institute of Research on the Structure of Matter, Chinese Academy of Sciences, Fuzhou, 350002, People's Republic of China

[§]Department of Chemistry, Faculty of Science, King Abdulaziz University, Jeddah, 21589, Saudi Abrabia

[‡]Graduate School of the Chinese Academy of Sciences, Beijing, 100049, People's Republic of China

Supporting Information

ABSTRACT: Reaction of europium sulfate octahydrate with *p*-terphenyl-3,3″,5,5″-tetracarboxylic acid (H_4ptptc) in a mixed solvent system has afforded three new coordination polymers formulated as $\{[Eu(ptptc)_{0.75}(H_2O)_2]\cdot 0.5DMF\cdot 1.5H_2O\}_n$ (**1**), $\{[Me_2H_2N]_2\ [Eu_2(ptptc)_2(H_2O)(DMF)]\cdot 1.5DMF\cdot 7H_2O\}_n$ (**2**), and $\{[Eu(Hptptc)(H_2O)_4]\cdot 0.5DMF\cdot H_2O\}_n$ (**3**). Complex **1** exhibits a three-dimensional (3D) metal−organic framework based on $\{Eu_2(\mu_2\text{-}COO)_2(COO)_4\}_n$ chains, complex **2** shows a 3D metal−organic framework constructed by $[Eu_2(\mu_2\text{-}COO)_2(COO)_6]^{2-}$ dimetallic subunits, and complex **3** features a 2D layer architecture assembling to 3D framework through $\pi\cdots\pi$ interactions. All complexes exhibit the characteristic red luminescence of Eu(III) ion. The triplet state of ligand H_4ptptc matches well with the emission level of Eu(III) ion, which allows the preparation of new optical materials with enhanced luminescence properties. The luminescence properties of these complexes are further studied in terms of their emission quantum yields, emission lifetimes, and the radiative/nonradiative rates.

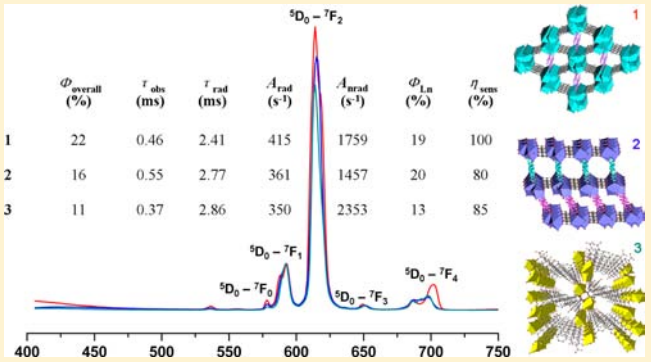

	$\Phi_{overall}$ (%)	τ_{obs} (ms)	τ_{rad} (ms)	A_{rad} (s^{-1})	A_{nrad} (s^{-1})	Φ_{Ln} (%)	η_{sens} (%)
1	22	0.46	2.41	415	1759	19	100
2	16	0.55	2.77	361	1457	20	80
3	11	0.37	2.86	350	2353	13	85

INTRODUCTION

Lanthanide complexes are the most popular luminescent materials for the applications in lasers, optical amplifiers, light-emitting diodes, and luminescent biosensing applications,[1] benefiting from the sharp and long lifetime characteristic 4f−4f emission bands, which result from the shielding of the $5s^25p^6$ filled subshells.[2] Especially, europium complexes have been regarded as attractive for using as luminescent materials because of their red emissions.[3] In general, the transitions between states within the $4f^n$ configuration are parity-forbidden and consist mainly of weak dipole (MD) and induced electric dipole (ED) transitions.[4] The intensities of the MD transitions are practically not influenced by the chemical surroundings of the ions, whereas those of the ED transitions are quite sensitive to it, according to Judd−Ofelt theory.[5] The characteristic emissions of europium complexes mainly come from ED transitions forbidden by Laporte's rule, because they correlate with the change of parity. However, transitions become partially allowed as a result of *J*-mixing and of the admixture of vibrational states or the states from the surrounding ligand field by introducing the organic ligand functioning as sensitizer to overcome the weak absorption induced by those forbidden rules.[6] In this regard, several chromophoric antenna ligands, especially the *β*-diketonate[7] and carboxylate ligands,[8] which have received the most attention, have been developed in an effort to achieve brighter lanthanide luminescence.

As demonstrated in the development of coordination polymers, the exploitation of new organic linkers plays a vital role in constructing coordination polymers with superior properties. Tetracarboxylate ligands, possessing four potential coordinationg groups, have been used as ideal organic linkers for building coordination polymers.[9] Considering the carboxylate groups interacting strongly with the oxophilic lanthanide ions, as well as the stability of the lanthanide carboxylates, which have attracted considerable attention for their potential use in a wide variety of fields, we were thus intrigued to explore the luminescence properties of the Eu(III) complexes by inclusion of a novel carboxylate ligand *p*-terphenyl-3,3″,5,5″-tetracarboxylic acid (H_4ptptc) for the first time. This ligand possesses delocalized *π*-electron system and can provide a strong absorbing sensitizer. Robustness and a certain degree of rigidity from the aromaticity of the terphenyl moiety are also useful in accessing a rigid and protective coordination shell to minimize nonradiative deactivation. In this contribution, we report the syntheses and structural characterization of {[Eu-

Received: March 28, 2013
Published: June 17, 2013

   dx.doi.org/10.1021/ic400777c | *Inorg. Chem.* 2013, 52, 7658−7665

$(ptptc)_{0.75}(H_2O)_2]\cdot 0.5DMF\cdot 1.5H_2O\}_n$ (**1**), $\{[Me_2H_2N]_2[Eu_2(ptptc)_2(H_2O)(DMF)]\cdot 1.5DMF\cdot 7H_2O\}_n$ (**2**), and $\{[Eu(Hptptc)(H_2O)_4]\cdot 0.5DMF\cdot H_2O\}_n$ (**3**). All structures of the newly synthesized complexes have been elucidated by single-crystal X-ray diffraction, powder X-ray diffractometry (PXRD), infrared (IR) spectroscopy, thermogravimetric analysi (TGA), and elemental analysis. The photophysical properties of these complexes have been investigated in terms of emission quantum yields, emission lifetimes, and the radiative/nonradiative rates, as well as the mechanism of energy transfer correlated with triplet energy levels of the ligand determined from the 77 K emission spectrum of its corresponding Gd(III) complexes.

EXPERIMENTAL SECTION

Materials and Methods. All reagents and solvents were purchased commercially and used without further purification. Elemental analyses (C, H, N, and O) were performed on a Elementar Vario MICRO elemental analyzer. IR spectra were recorded on KBr pellets in the 4000−400 cm^{-1} range using a Perkin−Elmer Spectrum One FT-IR spectrometer. Thermogravimetry−mass spectrometric analyses (TG-MS) were carried out in the temperature range of 30−1000 °C with a heating rate of 15 °C/min, using a Netzsch STA 449C simultaneous thermal analyzer coupled with mass spectrometry (Balzers MID). Powder X-ray diffraction (PXRD) patterns were collected on a Rigaku-D_{MAX} 2500 diffractometer with Cu Kα radiation (λ = 1.5406 Å). Diffuse reflectance spectra were obtained with a Perkin−Elmer Lambda-900 spectrophotometer equipped with an integrating sphere accessory ($BaSO_4$ was used as a reference). Steady-state photoluminescence spectra were recorded on a Horiba Jobin−Yvon Fluorolog-3 spectrophotometer analyzer, and the time-resolved luminescence was performed on an Edinburgh Instruments FLS920 spectrofluorometer equipped with both continuous (450 W) and pulse xenon lamps. The overall photoluminescence quantum yields were measured in solid state at room temperature, using a calibrated integrating sphere coated with barium sulfate.

Synthesis of $\{[Eu(ptptc)_{0.75}(H_2O)_2]\cdot 0.5DMF\cdot 1.5H_2O\}_n$ *(**1**).* H_4ptptc (0.0406 g, 0.1 mmol) and $Eu_2(SO_4)_3\cdot 8H_2O$ (0.1472 g, 0.2 mmol) were added to a 15-mL vial. A 1:1 (v/v) mixture of DMF and H_2O (8 mL) was added to the mixture. The content was sonicated for 15 min and then heated at 85 °C for 72 h to form colorless prism-shaped crystals, which were collected, washed with DMF, and dried in air with 68% yield, based on Eu. Anal. Calcd for $C_{18}H_{18}N_{0.5}O_{10}Eu_1$: C, 39.07; H, 3.28; N, 1.27; O, 28.92. Found: C, 39.24; H, 3.19; N, 1.31; O, 28.83. IR (KBr, cm^{-1}): 3410 (s), 2974 (w), 1615 (s), 1555 (s), 1451 (m), 1413 (m), 1384 (m), 833 (w), 765 (w), 733 (w).

Synthesis of $\{[Me_2H_2N]_2[Eu_2(ptptc)_2(H_2O)(DMF)_{0.5}]\cdot 1.5DMF\cdot 7H_2O\}_n$ *(**2**).* H_4ptptc (0.0406 g, 0.1 mmol), $Eu_2(SO_4)_3\cdot 8H_2O$ (0.1472 g, 0.2 mmol) and conc. H_2SO_4 (18 M; 0.05 mL) were added to a 15-mL vial. A 1:1 (v/v) mixture of DMF and H_2O (8 mL) was added to the mixture. The content was sonicated for 15 min and then heated at 85 °C for 72 h. The colorless hexagonal prism-like crystals were obtained, washed with DMF, and dried in air (73% yield based on Eu). Anal. Calcd for $C_{54}H_{66}N_4O_{26}Eu_2$: C, 43.50; H, 4.46; N, 3.76; O, 27.90. Found: C, 43.79; H, 4.32; N, 3.86; O, 27.48. IR (KBr, cm^{-1}): 3431 (s), 2972 (w), 1627 (s), 1454 (m), 1410 (m), 1383 (m), 783 (w), 778 (w), 734 (w).

Synthesis of $\{[Eu(Hptptc)(H_2O)_4]\cdot 0.5DMF\cdot H_2O\}_n$ *(**3**).* H_4ptptc (0.0406 g, 0.1 mmol), $Eu_2(SO_4)_3\cdot 8H_2O$ (0.1472 g, 0.2 mmol) and conc. H_2SO_4 (18 M; 0.05 mL) were added to a 15-mL vial. A 1:3 (v/v) mixture of DMF and H_2O (8 mL) was added to the solids. The content was sonicated for 15 min and then heated at 85 °C for 72 h. The colorless block-shaped crystals were obtained, washed with DMF, and dried in air (47% yield based on Eu). Anal. Calcd for $C_{23.5}H_{24.5}N_{0.5}O_{13.5}Eu_1$: C, 41.39; H, 3.62; N, 1.02; O, 31.67. Found: C, 41.10; H, 3.52; N, 0.98; O, 31.43. IR (KBr, cm^{-1}): 3422 (s), 2925 (w), 1622 (s), 1550 (s), 1450 (m), 1410 (m), 1384 (m), 785 (w), 757 (w), 761 (w).

X-ray Crystallographic Determination. The single-crystal structure data of three complexes were determined by Rigaku Mercury CCD area detector diffractometer equipped with graphite-monochromatic Mo Kα (λ = 0.71073 Å) radiation using the ω-scan mode at room temperature. Absorption corrections were applied by using the multiscan program SADABS.[10] All of the structures were resolved by the direct method and refined by full-matrix least-squares fitting on F^2 by SHELX-97.[11] All non-hydrogen atoms except some solvent molecules (badly disordered atoms) were refined with anisotropic thermal parameters. The positions of hydrogen atoms on the organic ligands were positioned geometrically (C−H bond length = 0.93 Å). The hydrogen atoms on water molecules were located in different density maps and refined as riding mode using the instruction AFIX 3, no attempt was made to locate the hydrogen atoms of disordered water molecules. All hydrogen atoms on solvent molecules were directly included in the molecular formulas. Thermal motions of DMF molecule were restrained by ISOR, DELU and SIMU, DFIX restraint was also used for reasonable bond distances of disordered DMF molecules. It should be noted that the solvent molecules (counterions, water and DMF) in the channels of complex **2** are highly disordered and could not be modeled properly, so the diffuse electron densities resulting from them are removed by the PLATON/SQUEEZE[12] to produce a set of solvent-free diffraction intensities. The SQUEEZE calculation shows a total solvent accessible area volume of 1305.2 $Å^3$ and the residual electron density amounted to 181 e per formula unit (Z = 2), corresponding to nearly two dimethylammonium cations, one and a half (1.5) DMF and seven (7) water molecules, which are also confirmed by elemental analysis, TG-MS analysis. We confirmed the CIF data by using the checkCIF/PLATON service. CCDC reference numbers are 899414 (**1**), 899418 (**2**) and 899415 (**3**), respectively. The summary of crystallographic data and structure refinements for **1**−**3** are listed in Table S1 in the Supporting Information. The selected bond lengths and angles of complexes **1**, **2**, and **3** are listed in Tables S2, S3, and S4 in the Supporting Information, respectively.

DISCUSSION

Syntheses and Structures. In order to investigate the photophysical properties of europium coordination polymers with same components, three europium−-tetracarboxylate coordination polymers were successfully synthesized under solvothermal condition. Considering the reaction process and the formation of final structure, which are well-affected by spatial coordinated disposition of the ligands, the stereo-electronic preference of the metal ions, metal−ligand ratios, temperatures, solvents, and counterions, here, the same amount of reactants of H_4ptptc and $Eu_2(SO_4)_3\cdot 8H_2O$ were used under DMF/H_2O solvothermal condition at 85 °C. Complexes **1**−**3** were finally obtained by addition of Lewis acid or varying the radio of the solvents. Single-crystal X-ray diffraction analyses reveal complexes **1** and **2** are 3D frameworks. In addition, complex **2** forms a three-dimensional (3D) supramolecular structure through $\pi\cdots\pi$ interactions based on 2D sheet architecture. The structural evidence demonstrates that ligand H_4ptptc is capable of binding the trivalent europium ion with carboxylate oxygen atoms in different coordination modes, to prepare metal−organic frameworks with diverse structures.

Crystal Structure of $\{[Eu(ptptc)_{0.75}(H_2O)_2]\cdot 0.5DMF\cdot 1.5H_2O\}_n$ *(**1**).* Single-crystal X-ray diffraction analysis reveals that complex **1** crystallizes in an orthorhombic *Fddd* space group, and exhibits a 3D structure constructed of discrete $\{Eu_2(\mu_2\text{-}COO)_2(COO)_4\}_n$ chains. As shown in Figure 1, the coordination geometry around the metal center can be described as a distorted triangular dodecahedron with four μ_2-bridging carboxylate oxygen atoms, two chelating carboxylate oxygen atoms, and two terminal water molecules to complete the coordination sphere. The Eu−O bond lengths fall

dx.doi.org/10.1021/ic400777c | Inorg. Chem. 2013, 52, 7658−7665

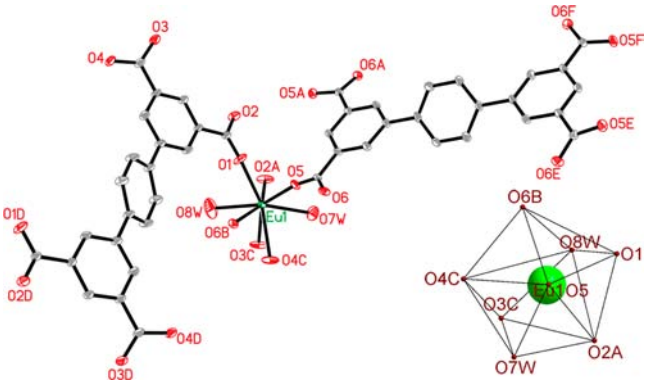

Figure 1. The coordination environment of Eu(III) ion in **1** with 30% thermal ellipsoids. All hydrogen atoms and solvent molecules are omitted for clarity. Inset: coordination polyhedron of Eu(III) ion. (Symmetry codes: A, $^1/_4 - x, y, ^1/_4 - z$; B, $^3/_4 - x, ^3/_4 - y, z$; C, $^1/_4 + x, ^1/_2 - y, -^1/_4 + z$; D, $1 - x, ^1/_2 - y, ^1/_2 - z$; E, $x, ^5/_4 - y, ^1/_4 - z$; F, $^1/_4 - x, ^5/_4 - y, z$.)

in the region of 2.298(3)−2.561(3) Å corresponding to those reported for other europium−oxygen donor complexes.[13] Eu1 and its corresponding symmetry generated atoms are linked through the bridging bidentate carboxylate groups to generate a europium-carboxylate chain $\{Eu_2(\mu_2\text{-}COO)_2(COO)_4\}_n$ propagating along the [100] direction, as illustrated in Figure 2a. The distances of Eu···Eu are 4.847 and 5.573 Å, respectively. The symmetry-generated ligands are associated with two types of coordination modes: μ_8-coordination type with four bridging bidentate carboxylate groups and μ_6-coordination type with two bridging bidentate and two chelating bidentate carboxylate groups. Detailed coordination modes of the ligands are shown in Figure S1 in the Supporting Information. The ligands with μ_8-coordination mode join the discrete chains together to produce a 3D framework with rhombic-shaped channels along the [100] direction (Figure 2b), while the ligands with μ_6-coordination mode occupy the channels and reinforce the framework as depicted in Figure 2c. The guest molecules reside in the channels forming O−H···O hydrogen-bonding interactions.

Crystal Structure of $\{[Me_2H_2N]_2[Eu_2(ptptc)_2(H_2O)(DMF)_{0.5}]\cdot 1.5DMF\cdot 7H_2O\}_n$ ***(2).*** Single-crystal X-ray diffraction analysis reveals that complex **2** crystallizes in a triclinic system $P\bar{1}$ space group and consists of a 3D anionic network based on $[Eu_2(\mu_2\text{-}COO)_2(COO)_6]^{2-}$ dimetallic subunits. The anionic framework is balanced by dimethylammonium counterions formed in situ upon heating of DMF through the well-established decarbonylation reaction.[14] As shown in Figure 3,

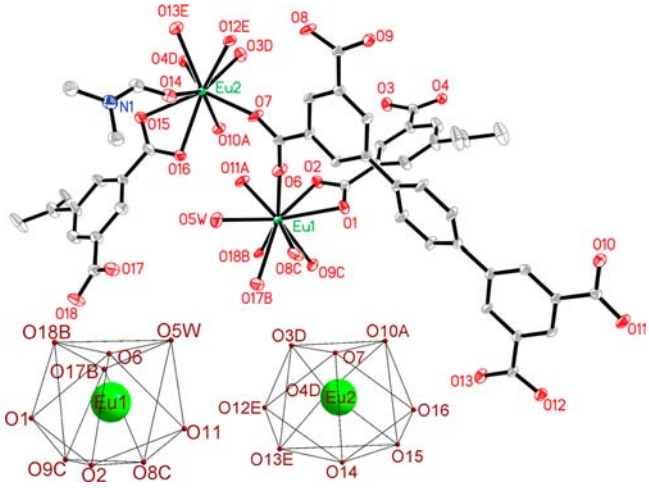

Figure 3. The coordination environments of Eu1 and Eu2 in **2** with 30% thermal ellipsoids. All hydrogen atoms and solvent molecules are omitted for clarity. Inset: coordination polyhedron of Eu(III) ions. (Symmetry codes: A, $x, 1 + y, z$; B, $1 - x, 2 - y, -z$; C, $1 + x, y, z$; D, $-x, 2 - y, 1 - z$; E, $x - 1, 1 + y, z$).

two crystallographically independent nine-coordinated Eu(III) ions are linked through a pair of *syn*−*syn* carboxylate bridges to form dimetallic units, with Eu···Eu distance being 5.569 Å. Individual dimetallic clusters are further cross-linked into a 3D framework by the spacer ligands. The coordination environments of two metal centers are similar, featuring distorted tricapped trigonal prism defined by six chelating carboxylate oxygen atoms, two bridging carboxylate oxygen atoms, with the remnant coordination sites of Eu1 occupied by one water and Eu2 by one DMF molecule. The Eu−O bond lengths vary from 2.306(5) Å to 2.589(5) Å, which are consistent with those analogous complexes.[15] There exist two types of coordination modes of $ptptc^{4-}$ ligand in complex **2**: μ_6-coordination style with two bridging bidentate and two chelating bidentate carboxylate groups and the μ_4-coordination style with four

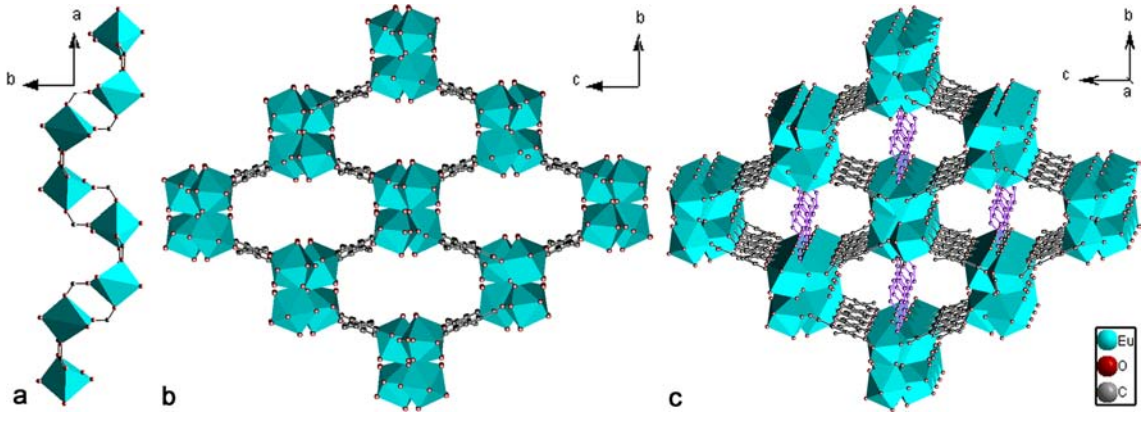

Figure 2. (a) The 1D $\{Eu_2(\mu_2\text{-}COO)_2(COO)_4\}_n$ chain of **1** along the [100] direction. (b) The projection of 3D framework in **1** at the (100) plane pillared by the ligands with μ_8-coordination mode. (c) The projection of 3D framework in **1** at the (100) plane sustained by the ligands. (The ligands with μ_6-coordination mode are shown in purple.)

dx.doi.org/10.1021/ic400777c | *Inorg. Chem.* 2013, 52, 7658−7665

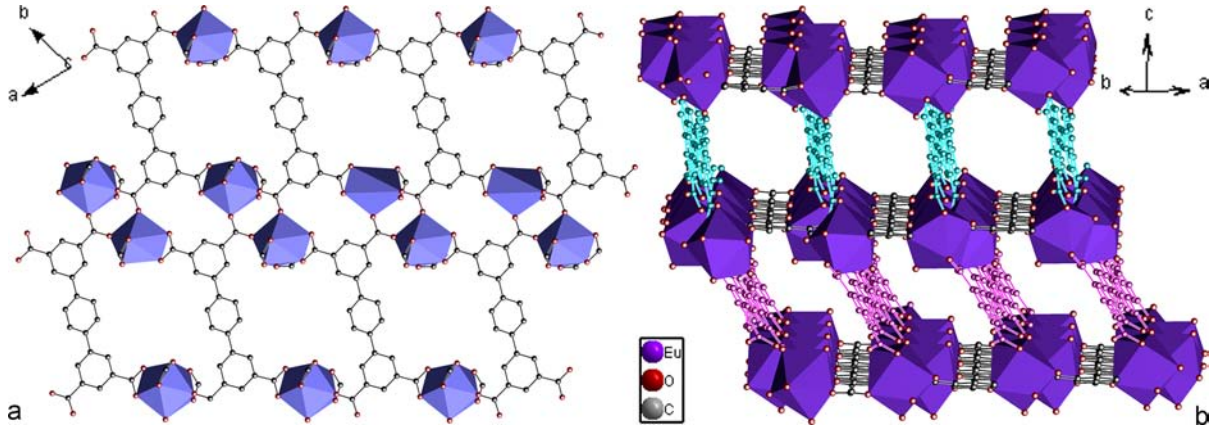

Figure 4. (a) The 2D layer of **2** constructed for 3D framework propagating along the (001) plane. (b) The projection of 3D framework of **2** (the different ligands with μ_4-coordination mode are presented in blue and pink, respectively).

chelating bidentate carboxylate groups. As shown in Figure 4a, each $[Eu_2(\mu_2\text{-}COO)_2(COO)_6]^{2-}$ dimetallic unit is surrounded by four ligands with μ_6-coordination mode that link the adjacent dimetallic units into a 2D network lying on (001) plane. The other ligands with μ_4-coordination mode cross-link the parallel layers upward and downward to pillar a 3D architecture containing 1D tetragonal channels where counterionic dimethylammonium, coordinated and lattice solvent molecules are located (Figure 4b).

*Crystal Structure of {[Eu(Hptptc)(H$_2$O)$_4$]·0.5DMF·H$_2$O}$_n$ (**3**).* Single X-ray diffraction (XRD) analysis reveals that complex **3** crystallizes in the triclinic $P\bar{1}$ space group, displaying a 3D stacking framework based on double-loop chains. As shown in Figure 5, the coordination geometry around the metal center

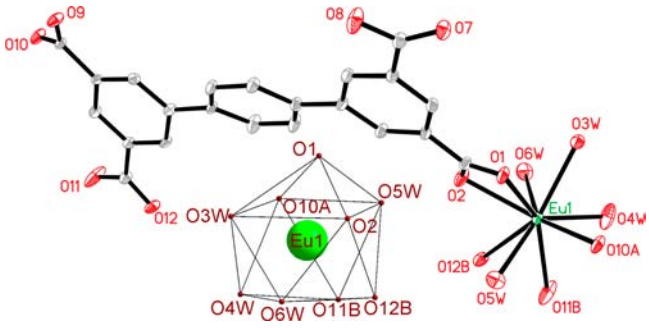

Figure 5. The coordination environment of Eu(III) in **3** with 30% thermal ellipsoids. All hydrogen atoms and solvent molecules are omitted for clarity. Inset: coordination polyhedron of Eu(III) ion. (Symmetry codes: A, $1 + x, y, z - 1$; B, $1 - x, -y, 1 - z$.)

can be described as a distorted capped square antiprism which defined by five carboxylate oxygen atoms from three different ligands and four oxygen atoms from terminal water molecules. The Eu–O bond lengths are consistent with those analogous reported, ranging from 2.267(3) Å to 2.581(3) Å.[16] The ligand adopts a μ_3-coordination mode, with two chelating bidentate and one monodentate fashions of carboxylate groups, while its uncoordinated carboxylate group is protonated for charge balance. The Eu(III) center and its symmetry generated one are aggregated by four chelating bidentate carboxylate groups of two ligands, leading to a ring structure. Adjacent rings are then linked into an infinite double-loop chain via the monodentate oxygen atom from free carboxylate of ring moiety, as illustrated in Figure 6a. The Eu···Eu separations in such chains are 6.007 and 12.269 Å. As depicted in Figure 6b, aromatic moieties in

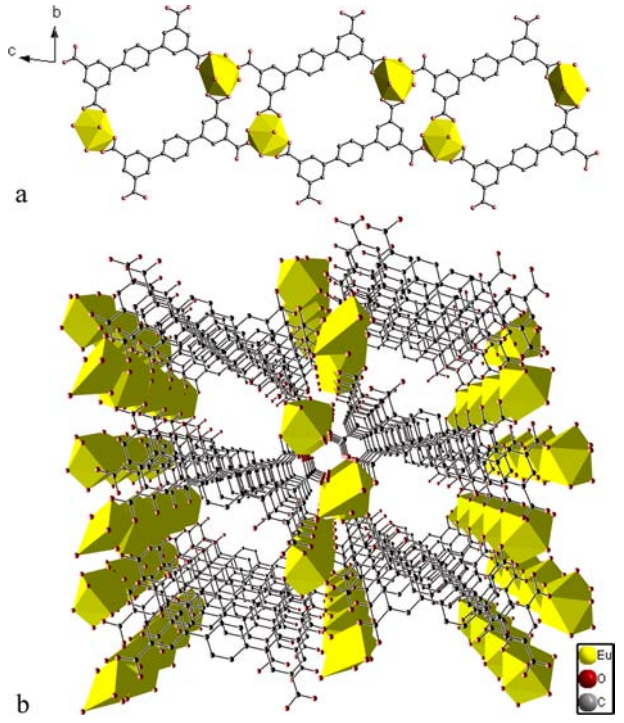

Figure 6. (a) The one-dimensional (1D) double-loop chain structure of **3**. (b) The projection of 3D framework constructed by π–π interactions in **3** at the (100) plane.

each chain are almost planar and array in a sliding mode. Further extension of structure through $\pi\cdots\pi$ interactions produces a 3D stacking network with the centroid–centroid distances being 3.771, 3.774, 3.986, 4.126, and 4.128 Å, respectively (Figure 7). This π-stacking plays an important role to stabilize the packing of such low-dimensional lattices, with stabilization effect being probably the same as those seen in discrete pillared 3D framework in complexes **1** and **2**, even though large pores occupied by interstitial solvents are present.

Thermal Stability and Powder X-ray Diffraction. The thermal stability of complexes **1**–**3** in the temperature range of 30–1000 °C under N_2 atmosphere is depicted in Figure S2 in the Supporting Information. TGA curves of three complexes

dx.doi.org/10.1021/ic400777c | Inorg. Chem. 2013, 52, 7658–7665

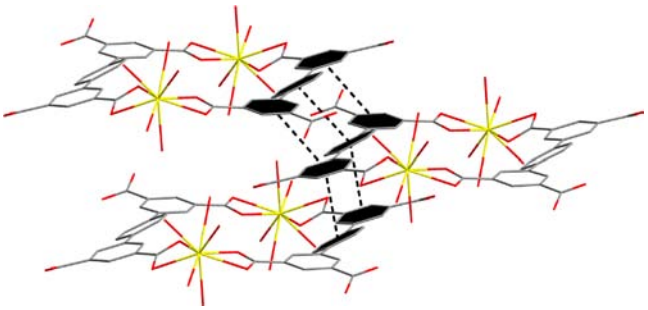

Figure 7. The $\pi-\pi$ interaction modes of each ring in double-loop chain in complex **3**.

exhibit two main weight loss steps, similarly corresponding to the loss of solvent water and DMF molecules until the decomposition of the framework. Complex **1** undergoes two steps of mass loss: the first step (found, 4.89%) at 30−90 °C corresponds to the loss of 1.5 lattice water molecules (theoretical, 4.88%); the second step (found 9.24%; theoretical, 9.86%), in the range of 90−430 °C, is attributed to the liberation of 0.5 lattice DMF molecule, after which the decomposition occurs to the remaining framework. In the case of complex **2**, 7 lattice water molecules are gradually released after heating to 100 °C with 8.08% weight loss found in the TGA curve (theoretical, 8.46%). The discrepancy of the found and theoretical values probably can be due to the loss of the lattice water at room temperature. Upon further heating to 380 °C, 1.5 lattice DMF molecules are released with 7.35% weight loss (theoretical, 7.18%). The host framework begins to decompose after further heating. The thermal decomposition process in complex **3** also proceeds in two steps. The first weight loss of 13.43% between 30 °C and 160 °C corresponds to the gradual loss of 1 lattice and 4 coordinated water molecules (theoretical, 13.21%). The rest of the stage with 5.95% mass loss can be assigned to the departure of 0.5 lattice DMF molecule until 400 °C (theoretical, 5.36%), then the remaining framework starts to collapse. The associated mass spectrometry m/z 18 (H_2O), m/z 73 (DMF) curves (Figure S2 in the Supporting Information) are in consistent with those of TGA analyses.

The purities of the bulky crystalline samples were confirmed by PXRD. The PXRD patterns of complexes **1**−**3** are illustrated in Figure S3 in the Supporting Information, which are in good agreement with simulated ones, confirming the phase purity of the as-synthesized products.

Electronic Spectra of the Ligand. The UV−vis diffuse reflectance spectra of free ligand and those of the corresponding Eu(III) complexes **1**−**3** were recorded in the solid state and displayed in Figure S4 in the Supporting Information. The absorption band at 321 nm for H_4ptptc can be attributed to the singlet−singlet $n \rightarrow \pi^*$ or $\pi \rightarrow \pi^*$ electronic transitions. The trends in the absorption band of the corresponding complexes are identical to those observed for the free ligand, indicating that the singlet excited state of the ligand is not significantly affected by the complexation of the Eu(III) ion. However, this complexation causes diminishment of the conjugation of ligands of Eu(III) complexes, indicated by the blue shift of ∼10 nm.[17]

The energy migration process is often discussed and modeled in terms of ligand-centered absorptions followed by the $^1S^* \rightarrow {}^3T^*$ intersystem crossing, $^3T^* \rightarrow Ln^*$ transfer, and Ln*-centered emission. Thus, for a ligand to be a good sensitizer, its donor state (usually, the lowest triplet state) should be situated sufficiently above the $^5D_0$ emitting level (17 500 cm^{-1}) or the $5D_1$ level (19 000 cm^{-1}) to allow efficient energy transfer and prevent quenching via the back energy transfer of $^5D_0$ or $^5D_1$ states.[18] Therefore, it becomes an important issue to determine the triplet state energy of the ligand, which can be calculated by referring to the lower wavelength emission edge of the corresponding phosphorescence spectrum of the Gd(III) complex.[7b,19] It is considered that Gd(III) complex is the optimum because the $^6P_{7/2}$ state of Gd(III) lies at too high energy to be populated through most organic ligands. In addition, the combination of both paramagnetic and heavy-atom effects facilitates the probability of ligand phosphorescence. Overall, the triplet energy of ligand H_4ptptc determined for the first time in complex $\{[Me_2H_2N]_2[Gd_2(ptptc)_2(H_2O)(DMF)_{0.5}]\cdot x DMF\cdot y H_2O\}_n$[20] (see Figure S5 in the Supporting Information) is 21 230 cm^{-1} that is lying ∼4000 cm^{-1} above the $^5D_0$ emitting state of the Eu(III) ion, and is suitable for sensitizing the luminescence of the Eu(III) ion. Therefore, all of the complexes display bright red luminescence, because of the characteristic $^5D_0-{}^7F_J$ (J = 0−4) transitions.

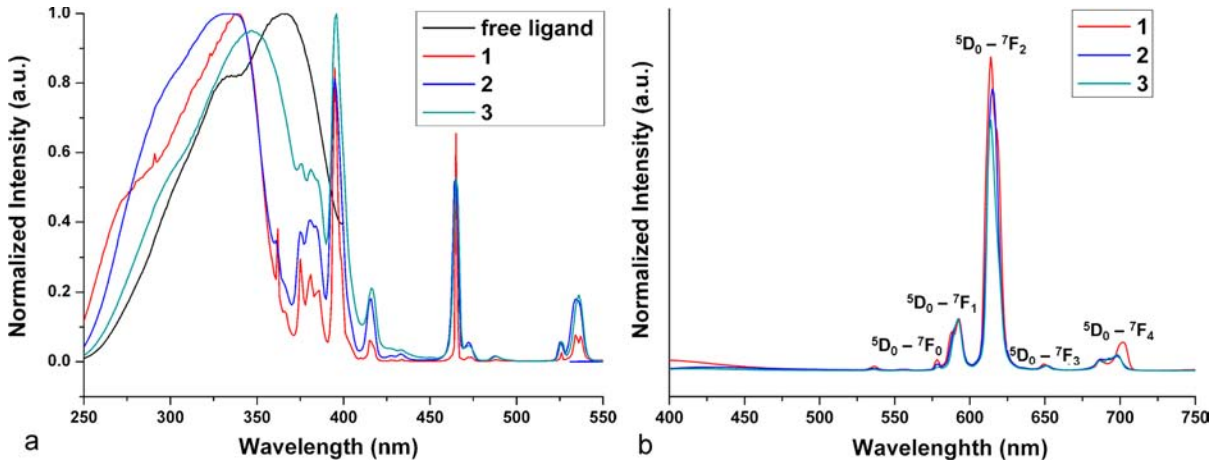

Figure 8. (a) Excitation spectra of the free ligand and complexes **1**−**3**. (b) Emission spectra of the complexes **1**−**3** excited at 350 nm. The spectra were normalized with respect to the magnetic dipole transition ($^5D_0 \rightarrow {}^7F_1$).

dx.doi.org/10.1021/ic400777c | Inorg. Chem. 2013, 52, 7658−7665

The Solid-State Luminescent Properties of Eu(III) Complexes. The room-temperature excitation spectra of the free ligand and Eu(III) complexes **1**−**3** recorded by monitoring the strongest emissions in the solid state are shown in Figure 8a. They all exhibit a broad band between 260 nm and 380 nm, which can be attributed to the $n \rightarrow \pi^*$ or $\pi \rightarrow \pi^*$ electronic transitions of ligand H_4ptptc. Each excitation profile of the complexes **1**−**3** mimics that of its corresponding ligand absorption spectrum in the range of 260−380 nm with a small blue shift, thus demonstrating that energy transfer occurs from the ligand H_4ptptc to the Eu(III) center. Meanwhile, a series of sharp lines characteristic of the Eu energy level structure are also observed in the excitation spectra of all complexes, which can be assigned to the transitions between $^7F_0$ and $^5L_6$ states, and transitions between $^7F_{0,1}$ and $^5D_{2,1}$ states.

Figure 8b presents the emission spectra recorded for all the complexes under ligand excitation (350 nm). These emission spectra show typical Eu red emissions in similar patterns, and exhibit well-resolved peaks centered at ∼578, 592, 614, 650, and 702 nm, corresponding to the transitions from the metal-centered $^5D_0$ excited state to the ^7F_J (J = 0−4) ground state multiplet with the hypersensitive $^5D_0 \rightarrow {}^7F_2$ transition dominating the spectra. No broad and strong emission band resulting from the ligand is observed, which demonstrates the ligand transfers the absorbed energy effectively to the emitting level of the Eu(III) center. As aforementioned, the magnetic dipole transition $^5D_0 \rightarrow {}^7F_1$ is independent of the environment, so it is used as an "internal reference" to probe the intensity of the induced electric dipole $^5D_0 \rightarrow {}^7F_2$ transition.

Time-resolved luminescence study was performed by monitoring the most intense emission lines within the $^5D_0 \rightarrow {}^7F_2$ transition at ambient temperature (298 K) under the excitation of the ligand band. Observed luminescence decays (see Figure S6 in the Supporting Information) for **1** and **3** could be fitted with a monoexponential function while the decay for **2** was a biexponential, consistent with the observation of two independent crystallographic sites for Eu(III).[21] The pertinent values of luminescence lifetime are summarized in Table 1.

Table 1. Overall Quantum Yields ($\Phi_{overall}$), Observed Luminescence Lifetimes (τ_{obs}), Radiative Luminescence Lifetimes (τ_{rad}), Radiative (A_{rad}) and Nonradiative (A_{nrad}) Decay Rates, Intrinsic Quantum Yields (Φ_{Ln}), and Sensitization Efficiencies (η_{sens}) for Complexes 1−3

complex	$\Phi_{overall}$ (%)	τ_{obs} (ms)	τ_{rad} (ms)	A_{rad} (s^{-1})	A_{nrad} (s^{-1})	Φ_{Ln} (%)	η_{sens} (%)
1	22	0.46	2.41	415	1759	19	100
2	16	0.55[a]	2.77	361	1457	20	80
3	11	0.37	2.86	350	2353	13	85

[a]This value corresponds to τ_{av}, given by $\tau_{av} = (A_1\tau_1^2 + A_2\tau_2^2)/(A_1\tau_1 + A_2\tau_2)$; τ_1 = 0.57 ms (94%), τ_2 = 0.30 ms (6%).

Quantum yield is another important parameter characterizing the emission process of Eu(III) ions in addition to luminescence lifetime. To qualify the ability of the ligand H_4ptptc sensitizing the emission of Eu(III) center, and to get information of the relationship between the structures and photoluminescence properties, it was appropriate to analyze the ligand-sensitized overall quantum yield ($\Phi_{overall}$), intrinsic quantum yield (Φ_{Ln}), and the efficiency of the ligand-to-metal energy transfer (η_{sens}), depicted in terms of eq 1:[22]

$$\Phi_{overall} = \eta_{sens} \times \Phi_{ln} \quad (1)$$

The overall quantum yield can be obtained experimentally under excitation of the ligand. However experimental determination of the intrinsic quantum yield is difficult in view of the faint absorbance of f−f transitions, so this quantum yield is often calculated from eq 2,[23] where A_{rad} and A_{nrad} represent the radiative and nonradiative decay rates, and the τ_{obs}/τ_{rad} are the observed and radiative lifetimes of Eu($^5D_0$):

$$\Phi_{ln} = \frac{A_{rad}}{A_{rad} + A_{nrad}} = \frac{\tau_{obs}}{\tau_{rad}} \quad (2)$$

Therefore, the lifetime of the emitting state ($^5D_0$) τ_{obs}, and the radiative rate (A_{rad}) and the nonradiative rate (A_{nrad}) are related through

$$\frac{1}{\tau_{obs}} = A_{rad} + A_{nrad} \quad (3)$$

where A_{rad} rate is obtained by $A_{rad} = 1/\tau_{rad}$. The radiative lifetime of Eu($^5D_0$) τ_{rad} is considered to calculated by eq 4[23] to obtain the intrinsic quantum yield, in which $A_{MD,0}$ is the deactivation rate associated with the spontaneous emission probability for the $^5D_0 \rightarrow {}^7F_1$ transition in vacuo, equal to 14.65 s^{-1}; I_{tot}/I_{MD} is the ratio of the total integrated $^5D_0 \rightarrow {}^7F_J$ emissions (J = 0−4) to the magnetic dipole $^5D_0 \rightarrow {}^7F_1$ transition and the refractive index of the medium (n) is taken to be equal to 1.5 in the solid sample employed in the calculation that is commonly encountered for coordination complexes.

$$\frac{1}{\tau_{rad}} = A_{MD,0} \times n^3 \times \left(\frac{I_{tot}}{I_{MD}}\right) \quad (4)$$

Table 1 summarizes the $\Phi_{overall}$, τ_{obs} and other photophysical parameters. Although ligand H_4ptptc can sensitize the emissive Eu center with large sensitization efficiencies that depend on the energy gap between the lowest triplet energy level of ligand and the emissive energy level of the Eu ion, these Eu complexes exhibit small emission lifetimes and quantum yields. Generally, such long π-rich conjugated backbone ligand cannot occupy the entire coordination sphere of the Eu(III) ion, leaving some binding sites for solvent molecules used as the reacting medium. As a consequence, a vibronic coupling between Eu and OH oscillators occurs, which provides a facile nonradiative deactivation path for the Eu(III) ion. Such deactivation process leads to the small luminescence quantum yields and lifetimes, which is also proven by the large nonradiative rates.

Complex **1** exhibits a relatively large quantum yield and radiative decay rate constant, which is probably linked to the distorted 8-coordinate dodecahedron environment of the Eu(III) ion.[24] In this geometry, the $^5D_0 \rightarrow {}^7F_2$ hypersensitive transition is allowed by symmetry-related selection rules and becomes sizable. With respect to **1**, the nonradiative rate constant of **2** decreases by ∼17% which we attribute to the presence of only one water molecule in the inner coordination sphere, compared to two. On the other hand, both the radiative decay rate and the sensitization efficiency decrease, so that the overall quantum yield is smaller, compared to **1**. Finally, due to four bond water molecules in **3**, the nonradiative rate constant is 60% larger than for **2**, resulting in a concomitant decrease in the overall quantum yield. These data emphasize the significant negative impact of water on luminescent properties, so that the

dx.doi.org/10.1021/ic400777c | Inorg. Chem. 2013, 52, 7658−7665

design of highly luminescent compounds would require removing them from the inner coordination sphere.

CONCLUSION

In summary, three novel europium-tetracarboxylate coordination polymers have been successfully synthesized, structurally characterized, and optically studied. Single-crystal X-ray diffraction (XRD) analyses revealed that different coordination modes of the tetracarboxylate ligands with Eu ions could promote the formation of different final structures. Complexes **1** and **2** exhibit three-dimensional (3D) metal−organic frameworks based on $\{Eu_2(\mu_2\text{-}COO)_2(COO)_4\}_n$ chains or $[Eu_2(\mu_2\text{-}COO)_2(COO)_6]^{2-}$ dimetallic subunits, and complex **3** features a 2D layer architecture assembling into 3D framework through $\pi\cdots\pi$ interactions. The detail luminescent properties of complexes **1**−**3** in the solid state are investigated at room temperature. It is found that the Eu(III) ion could be highly sensitized by this π-rich ligand H_4ptptc, although the existence of an OH quenching effect makes the small luminescence lifetimes and quantum yields. The energy level of the triplet state of the ligand, determined from the phosphorescence at 77 K of the Gd(III) complex, is higher than the emissive level of Eu(III) ion, demonstrating the potential of H_4ptptc as an efficient UV light sensitizer for europium-based red emission. This work provides some insight into the correlation between structures and luminescence properties and, thus, can be useful in synthesizing desirable luminescent materials.

ASSOCIATED CONTENT

Supporting Information

The selected bond length and angle parameters of complexes **1**−**3**, PXRD patterns and TGA diagram for complexes **1**−**3**, and other supplementary figures of optical data. This material is available free of charge via the Internet at http://pubs.acs.org.

AUTHOR INFORMATION

Corresponding Author

*Tel.: +86 591 83792460. Fax: +86 591 83794946. E-mail: hmc@fjirsm.ac.cn.

Notes

The authors declare no competing financial interest.

ACKNOWLEDGMENTS

We are thankful for financial support from 973 Program (Nos. 2011CBA00507 and 2011CB932504), National Nature Science Foundation of China (No. 21131006), and Nature Science Foundation of Fujian Province.

REFERENCES

(1) (a) Binnemans, K. *Chem. Rev.* **2009**, *109*, 4283−4374. (b) Farinola, G. M.; Ragni, R. *Chem. Soc. Rev.* **2011**, *40*, 3467−3482. (c) Kido, J.; Okamoto, Y. *Chem. Rev.* **2002**, *102*, 2357−2368. (d) Kuriki, K.; Koike, Y.; Okamoto, Y. *Chem. Rev.* **2002**, *102*, 2347−2356. (e) Eliseeva, S. V.; Bunzli, J. C. G. *Chem. Soc. Rev.* **2010**, *39*, 189−227. (f) Kobayashi, H.; Ogawa, M.; Alford, R.; Choyke, P. L.; Urano, Y. *Chem. Rev.* **2009**, *110*, 2620−2640. (g) Sinkeldam, R. W.; Greco, N. J.; Tor, Y. *Chem. Rev.* **2010**, *110*, 2579−2619.

(2) (a) Werts, M. H. V. *Sci. Prog.* **2005**, *88*, 101−131. (b) Bunzli, J. C. G. *Acc. Chem. Res.* **2006**, *39*, 53−61. (c) Bunzli, J. C. G.; Piguet, C. *Chem. Soc. Rev.* **2005**, *34*, 1048−1077.

(3) (a) Huignard, A.; Gacoin, T.; Boilot, J. P. *Chem. Mater.* **2000**, *12*, 1090−1094. (b) Maggini, L.; Mohanraj, J.; Traboulsi, H.; Parisini, A.; Accorsi, G.; Armaroli, N.; Bonifazi, D. *Chem.—Eur. J.* **2011**, *17*, 8533−8537. (c) Shelton, A. H.; Sazanovich, I. V.; Weinstein, J. A.; Ward, M. D. *Chem. Commun.* **2012**, *48*, 2749−2751. (d) Cui, Y. J.; Xu, H.; Yue, Y. Y.; Guo, Z. Y.; Yu, J. C.; Chen, Z. X.; Gao, J. K.; Yang, Y.; Qian, G. D.; Chen, B. L. *J. Am. Chem. Soc.* **2012**, *134*, 3979−3982.

(4) (a) Chen, X. Y.; Liu, G. K. *J. Solid State Chem.* **2005**, *178*, 419−428. (b) Van Vleck, J. H. *J. Phys. Chem.* **1937**, *41*, 67−80.

(5) (a) Ofelt, G. S. *J. Chem. Phys.* **1962**, *37*, 511. (b) Judd, B. R. *Phys. Rev.* **1962**, *127*, 750.

(6) (a) Weissman, S. I. *J. Chem. Phys.* **1942**, *10*, 214−217. (b) de Lill, D. T.; de Bettencourt-Dias, A.; Cahill, C. L. *Inorg. Chem.* **2007**, *46*, 3960−3965. (c) Crosby, G. A.; Alire, R. M.; Whan, R. E. *J. Chem. Phys.* **1961**, *34*, 743. (d) Leonard, J. P.; Gunnlaugsson, T. *J. Fluoresc.* **2005**, *15*, 585−595. (e) Moore, E. G.; Samuel, A. P. S.; Raymond, K. N. *Acc. Chem. Res.* **2009**, *42*, 542−552.

(7) (a) Zucchi, G.; Murugesan, V.; Tondelier, D.; Aldakov, D.; Jeon, T.; Yang, F.; Thuery, P.; Ephritikhine, M.; Geffroy, B. *Inorg. Chem.* **2011**, *50*, 4851−4856. (b) Freund, C.; Porzio, W.; Giovanella, U.; Vignali, F.; Pasini, M.; Destri, S.; Mech, A.; Di Pietro, S.; Di Bari, L.; Mineo, P. *Inorg. Chem.* **2011**, *50*, 5417−5429.

(8) (a) Wang, P.; Ma, J. P.; Dong, Y. B.; Huang, R. Q. *J. Am. Chem. Soc.* **2007**, *129*, 10620−10621. (b) Monge, A.; Gandara, F.; Gutierrez-Puebla, E.; Snejko, N. *CrystEngComm* **2011**, *13*, 5031−5044. (c) Gai, Y. L.; Xiong, K. C.; Chen, L.; Bu, Y.; Li, X. J.; Jiang, F. L.; Hong, M. C. *Inorg. Chem.* **2012**, *51*, 13128−13137. (d) Marchal, C.; Filinchuk, Y.; Chen, X. Y.; Imbert, D.; Mazzanti, M. *Chem.—Eur. J.* **2009**, *15*, 5273−5288.

(9) (a) Lanthanide-containing coordination polymers in *Handbook on the Physics and Chemistry of Rare Earths*; Elsevier B.V.: Amsterdam, Vol. *34*, Ch. 221, pp 359−404. (b) Ji, B. M.; Deng, D. S.; He, X.; Liu, B.; Miao, S. B.; Ma, N.; Wang, W. Z.; Ji, L. G.; Liu, P.; Li, X. F. *Inorg. Chem.* **2012**, *51*, 2170−2177. (c) Sun, L. B.; Li, Y.; Liang, Z. Q.; Yu, J. H.; Xu, R. R. *Dalton Trans.* **2012**, *41*, 12790−12796. (d) Pan, Z. R.; Xu, J. A.; Yao, X. Q.; Li, Y. Z.; Guo, Z. J.; Zheng, H. G. *CrystEngComm* **2011**, *13*, 1617−1624. (e) Su, S. Q.; Chen, W.; Qin, C.; Song, S. Y.; Guo, Z. Y.; Li, G. H.; Song, X. Z.; Zhu, M.; Wang, S.; Hao, Z. M.; Zhang, H. J. *Cryst. Growth Des.* **2012**, *12*, 1808−1815. (f) Kelly, N. R.; Goetz, S.; Batten, S. R.; Kruger, P. E. *CrystEngComm* **2008**, *10*, 1018−1026.

(10) Sheldrick, G. M. *SADABS 2.05*; University of Göttingen: Göttingen, Germany, 2002.

(11) Sheldrick, G. M. *SHELXS-97, Programs for X-ray Crystal Structure Solution*; University of Göttingen: Göttingen, Germany, 1997.

(12) P. van der Sluis, A. L. S. *Acta Crystallogr., Sect. A: Found Crystallogr.* **1990**, *46*, 194−201.

(13) (a) Chen, M. S.; Su, Z.; Chen, M.; Chen, S. S.; Li, Y. Z.; Sun, W. Y. *CrystEngComm* **2010**, *12*, 3267−3276. (b) Dai, J. W.; Tong, M. L. *CrystEngComm* **2012**, *14*, 2124−2131. (c) Wang, P.; Ma, J. P.; Dong, Y. B. *Chem.—Eur. J.* **2009**, *15*, 10432−10445.

(14) (a) Burrows, A. D.; Cassar, K.; Duren, T.; Friend, R. M. W.; Mahon, M. F.; Rigby, S. P.; Savarese, T. L. *Dalton Trans.* **2008**, 2465−2474. (b) Xiong, K. C.; Jiang, F. L.; Gai, Y. L.; Zhou, Y. F.; Yuan, D. Q.; Su, K. Z.; Wang, X. Y.; Hong, M. C. *Inorg. Chem.* **2012**, *51*, 3283−3288.

(15) (a) Decadt, R.; Van Hecke, K.; Depla, D.; Leus, K.; Weinberger, D.; Van Driessche, I.; Van Der Voort, P.; Van Deun, R. *Inorg. Chem.* **2012**, *51*, 11623−11634. (b) Lucky, M. V.; Sivakumar, S.; Reddy, M. L. P.; Paul, A. K.; Natarajan, S. *Cryst. Growth Des.* **2011**, *11*, 857−864. (c) Cepeda, J.; Balda, R.; Beobide, G.; Castillo, O.; Fernandez, J.; Luque, A.; Perez-Yanez, S.; Roman, P. *Inorg. Chem.* **2012**, *51*, 7875−7888.

(16) (a) Liu, L. L.; Ren, Z. G.; Zhu, L. W.; Wang, H. F.; Yan, W. Y.; Lang, J. P. *Cryst. Growth Des.* **2011**, *11*, 3479−3488. (b) He, H.; Yuan, D.; Ma, H.; Sun, D.; Zhang, G.; Zhou, H. C. *Inorg. Chem.* **2010**, *49*, 7605−7607. (c) Huang, Y. G.; Wu, B. L.; Yuan, D. Q.; Xu, Y. Q.; Jiang, F. L.; Hong, M. C. *Inorg. Chem.* **2007**, *46*, 1171−1176.

(17) Li, H. F.; Yan, P. F.; Chen, P.; Wang, Y.; Xu, H.; Li, G. M. *Dalton Trans.* **2012**, *41*, 900−907.

(18) (a) Latva, M.; Takalo, H.; Mukkala, V. M.; Matachescu, C.; Rodriguez-Ubis, J. C.; Kankare, J. *J. Lumin.* **1997**, *75*, 149−169. (b) Sato, S.; Wada, M. *Bull. Chem. Soc. Jpn.* **1970**, *43*, 1955.

(19) (a) Eliseeva, S. V.; Pleshkov, D. N.; Lyssenko, K. A.; Lepnev, L. S.; Bunzli, J. C.; Kuzmina, N. P. *Inorg. Chem.* **2011**, *50*, 5137−5144. (b) Sivakumar, S.; Reddy, M. L.; Cowley, A. H.; Butorac, R. R. *Inorg. Chem.* **2011**, *50*, 4882−4891.

(20) Complex $\{[Me_2H_2N]_2[Gd_2(ptptc)_2(H_2O)(DMF)_{0.5}]\cdot x\text{DMF}\cdot yH_2O\}_n$ was synthesized in order to get the information about the triplet state of the ligand H_4ptptc. The synthesis process was same as complex **2**. Crystal data for squeezed complex $C_{45.5}H_{25.5}N_{0.5}O_{17.5}Gd_2$: M = 1173.66, triclinic, space group $P\bar{1}$, a = 10.949(3) Å, b = 16.078(4) Å, c = 19.650(5) Å, α = 74.633(12), β = 73.957(12), γ = 72.093(11)°, V = 3101.6(14) Å^3, Z = 2, T = 293(2) K, Dc = 1.257 g cm^{-3}, F(000) = 1140, Mo-$K\alpha$ radiation (λ = 0.71073 Å), R(int) = 0.0321, 24217 reflections collected, 14119 unique, μ = 2.174 mm^{-1}, $R1$ ($wR2$) = 0.0449 (0.1206) and $GooF$ = 1.076 for 11709 reflections with $I > 2\sigma(I)$.

(21) (a) Comby, S.; Scopelliti, R.; Imbert, D.; Charbonniere, L.; Ziessel, R.; Bunzli, J. C. G. *Inorg. Chem.* **2006**, *45*, 3158−3160. (b) Huang, Y. G.; Wu, B. L.; Yuan, D. Q.; Xu, Y. Q.; Jiang, F. L.; Hong, M. C. *Inorg. Chem.* **2007**, *46*, 1171−1176. (c) White, K. A.; Chengelis, D. A.; Zeller, M.; Geib, S. J.; Szakos, J.; Petoud, S.; Rosi, N. L. *Chem. Commun.* **2009**, 4506−4508. (d) Liu, T. F.; Zhang, W.; Sun, W. H.; Cao, R. *Inorg. Chem.* **2011**, *50*, 5242−5248.

(22) Xiao, M.; Selvin, P. R. *J. Am. Chem. Soc.* **2001**, *123*, 7067−7073.

(23) (a) Chauvin, A. S.; Gumy, F.; Imbert, D.; Bunzli, J. C. G. *Spectrosc. Lett.* **2007**, *40*, 193−193. (b) Chauvin, A. S.; Gumy, F.; Imbert, D.; Bunzli, J. C. G. *Spectrosc. Lett.* **2004**, *37*, 517−532.

(24) The coordination geometries around the Eu(III) centers were estimated by the continuous shape measure analysis,a carried out with Shape program based on the calculation of a set of atomic positions relative to the vertices of ideal polyhedra. The results of the Shape analyses are given in Table S5, and lowest value of continuous shape measure for three pairs represents the best fit to the closet idealized geometry. (a) Pinsky, M.; Avnir, D. *Inorg. Chem.* **1998**, *37*, 5575−5582.

dx.doi.org/10.1021/ic400777c | *Inorg. Chem.* 2013, 52, 7658−7665